Star Calibration Techniques using Ground-Based Narrow-band Imaging

Guy Grubbs II[1,2], Marilia Samara[3], Robert Michell[3,4], and Don Hampton[5]

1. University of Texas at San Antonio
2. Southwest Research Institute, San Antonio, TX
3. Goddard Space Flight Institute, Greenbelt, MD
4. University of Maryland, College Park, MD
5. University of Alaska, Fairbanks, AK

Scientific Motivation

- Standard units for each observation
  - Self-comparison and other missions
- Modeling comparison using absolute intensity
- Calibration factors available daily
  - Normally imagers must be removed from field
- Automated (systematic and mathematical) method

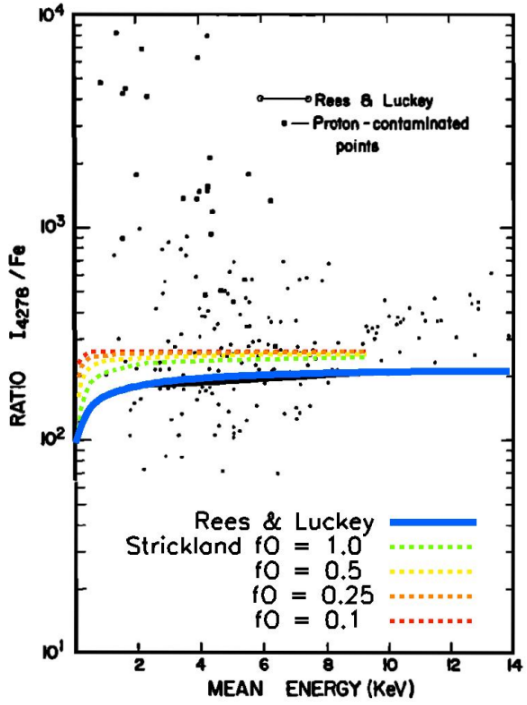

Kasting & Hays, 1977

Instrumental Setup

- Field of view (19, 47, and 180^{o} FoV)
- Readout rate (10 MHz max)
- Resolution (1024x1024 pixels @ 13 µm/side)
- Filters (2 nm passband)

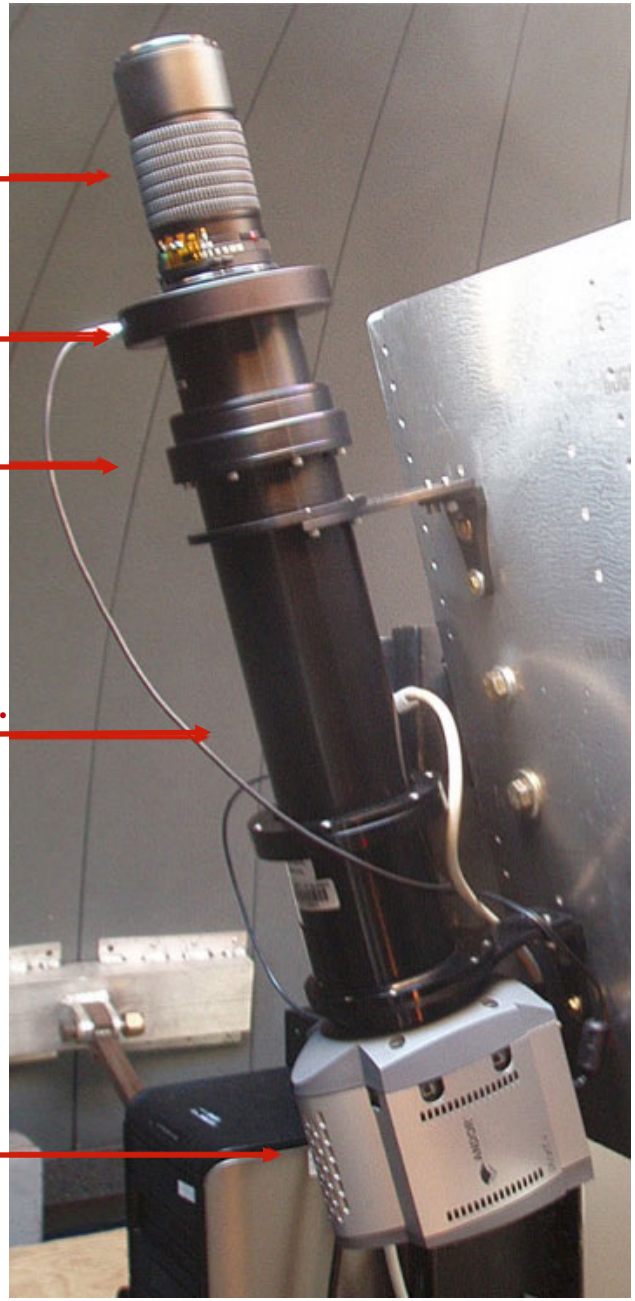

Star Mapping and Calibration

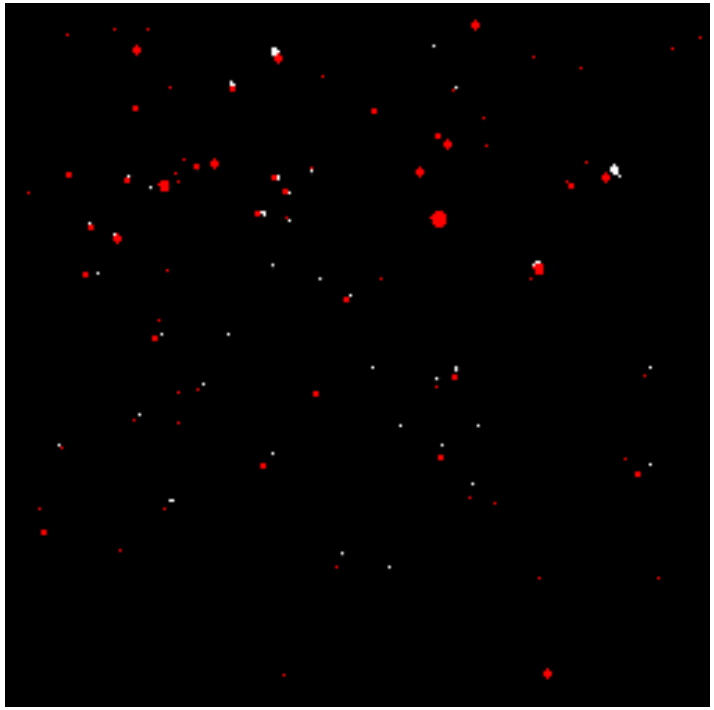

White = Observed
Red = Star Mapping Software
(thanks to UAF/Hampton)

	Pixel x,y		Rght Asc	Decl	mag	spectrum
5	157.7 180.7	(75.2)	05 12 59	45 56 58	0.21	64 G0
6	210.7 254.1	(1.8)	05 23 08	28 34 02	1.78	28 B8
7	59.1 190.8	(65.1)	03 20 44	49 41 06	1.90	48 F5
8	193.3 163.8	(92.1)	05 55 52	44 56 41	2.07	15 A0P
9	217.4 195.9	(60.0)	05 56 19	37 12 40	2.71	15 A0P
10	48.9 238.4	(17.5)	03 04 54	40 45 52	2.85	28 B8
11	170.0 249.0	(6.9)	04 53 44	33 05 20	2.90	90 K2
12	98.8 236.3	(19.6)	03 54 29	39 52 03	2.96	23 B1

Table G.7. Stellar data[a], Luminosity Class V (Dwarfs)

Spectral type	B–V	V–R	M_V	BC	T_{eff}(K)	$R/R_\odot$	$M/M_\odot$
O3				−4.3?	48000		50?
O5			−5?	−4.3?	44000		30?
O6	−0.32	−0.15	−4.8	−4.25	43000	12?	25?
O8	−0.31	−0.15	−4.1	−3.93	37000	10	20?
B0	−0.29	−0.13	−3.3	−3.34	31000	7.2	17
B1	−0.26	−0.11	−2.9	−2.6	24100	5.3	10.7
B2	−0.24	−0.1	−2.5	−2.2	21080	4.7	8.3
B3	−0.21	−0.08	−2	−1.69	18000	3.5	6.3
B4	−0.18	−0.07	−1.5	−1.29	15870	3	5
B5	−0.16	−0.06	−1.1	−1.08	14720	2.9	4.3
B8	−0.1	−0.02	0	−0.6	11950	2.3	3
A0	0	0.02	0.7	−0.14	9572	1.8	2.34
A2	0.06	0.08	1.3	0	8985	1.75	2.21
A5	0.14	0.16	1.9	0.02	8306	1.69	2.04
A7	0.19	0.19	2.3	0.02	7935	1.68	1.93

Irwin, 2007

$$f_{det}(\theta,A,t) = \int_0^\infty BB_{flux}(\lambda) * Atm(\lambda,\theta) * T_{filt}(\lambda) * QE(\lambda)\, d\lambda$$

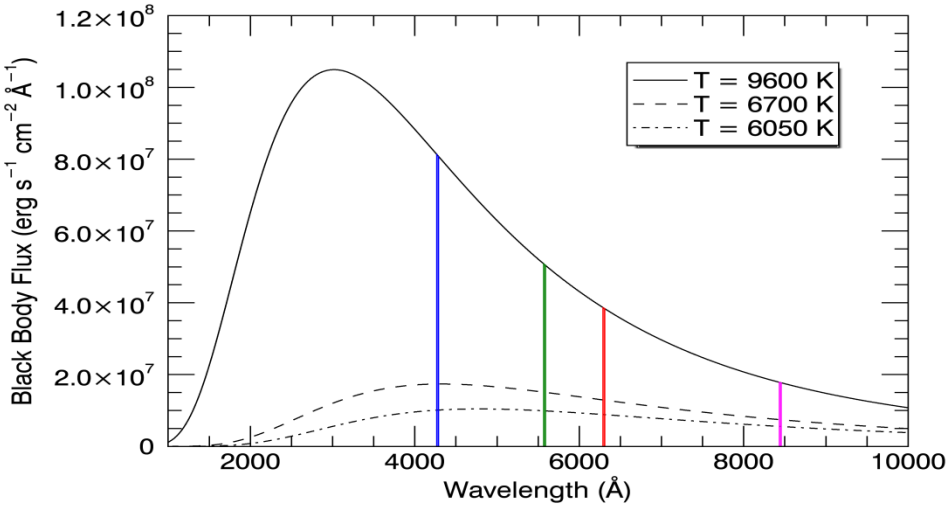

Assuming black-body radiation, the spectral photon irradiance from a star of apparent bolometric magnitude m_b is given by:

$$f(\lambda) = \frac{8.48 \times 10^{34} \times 10^{-0.4 m_b}}{T_e^4 \lambda^4 [\exp(1.44 \times 10^8 / \lambda T_e) - 1]} \quad \text{photons cm}^{-2}\,\text{s}^{-1}\,\text{Å}^{-1}$$

λ in Å; T_e the effective temperature of the star in K (e.g., A0 star; $m_V = 0$, $T_e = 10800$, $BC = -0.40$, $\lambda = 5000$ Å; $f(\lambda) = 10^3$ photons cm^{-2} s^{-1} Å^{-1}).

Zombeck, 2006

Atmospheric Effects:

- Extinction
- Transmission Coefficient
- Clouds
- "Seeing"

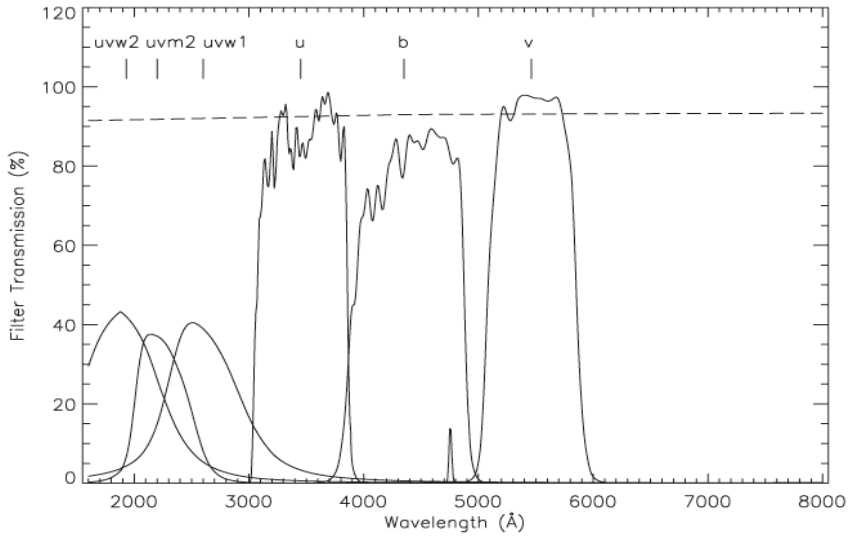

Poole et al., 2008

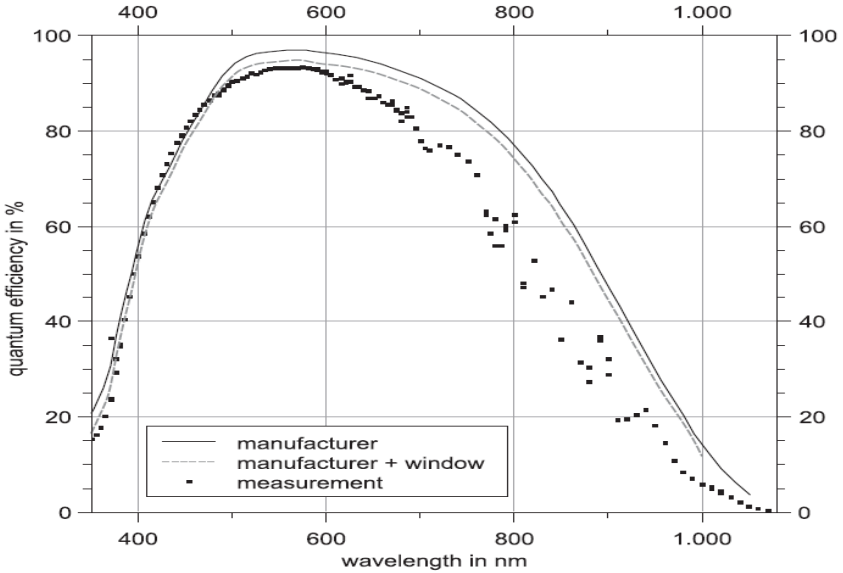

Sperlich and Stolz, 2013

Star Mapping and Calibration

Using star mapping for θ,
Area of aperture = π cm^2,
and 1 s exposure time:

$$f\downarrow det\ (\theta\downarrow star\ ,A,t)*\pi=C\downarrow \gamma$$

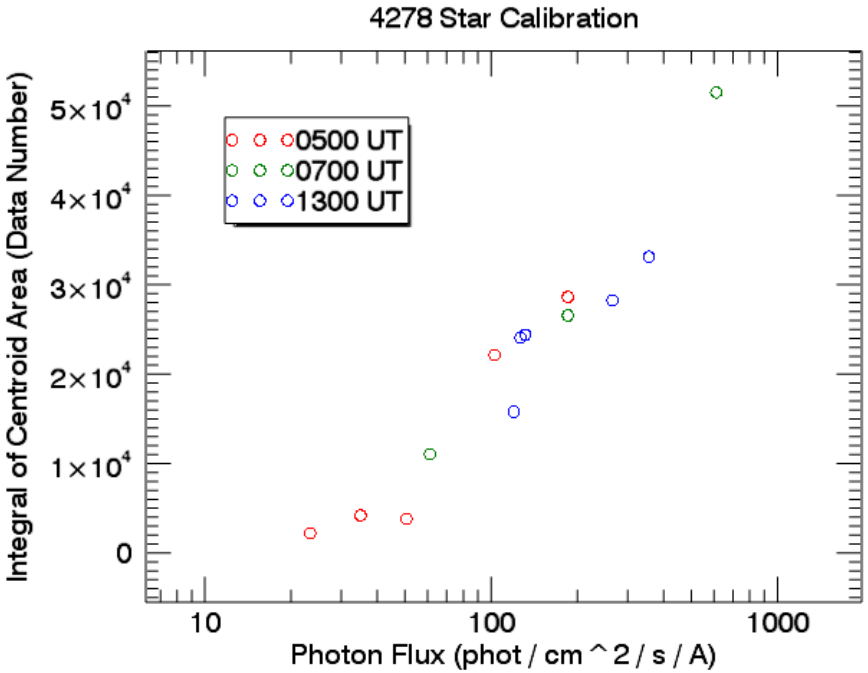

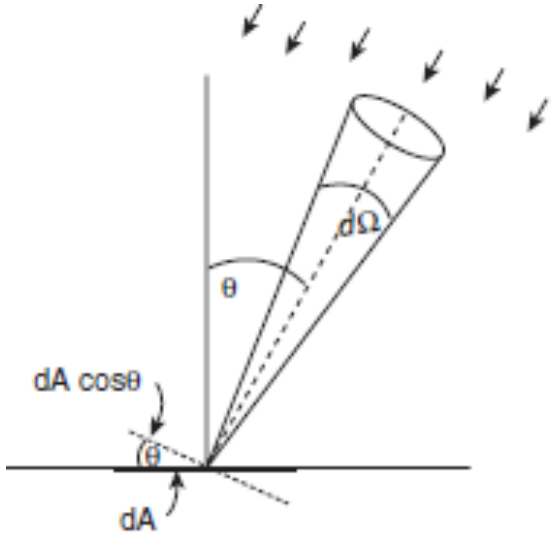

Field of View: 47° = .82 radians
$.82/256 = .0032$ radians to each side of the pixel.

Used to derive intensity in Rayleighs measured by each pixel.

Summary

- Star mapping needs improvement
- Technique needs to be fully automated
- Star calibration show lots of promise

Questions?

Backup Slides

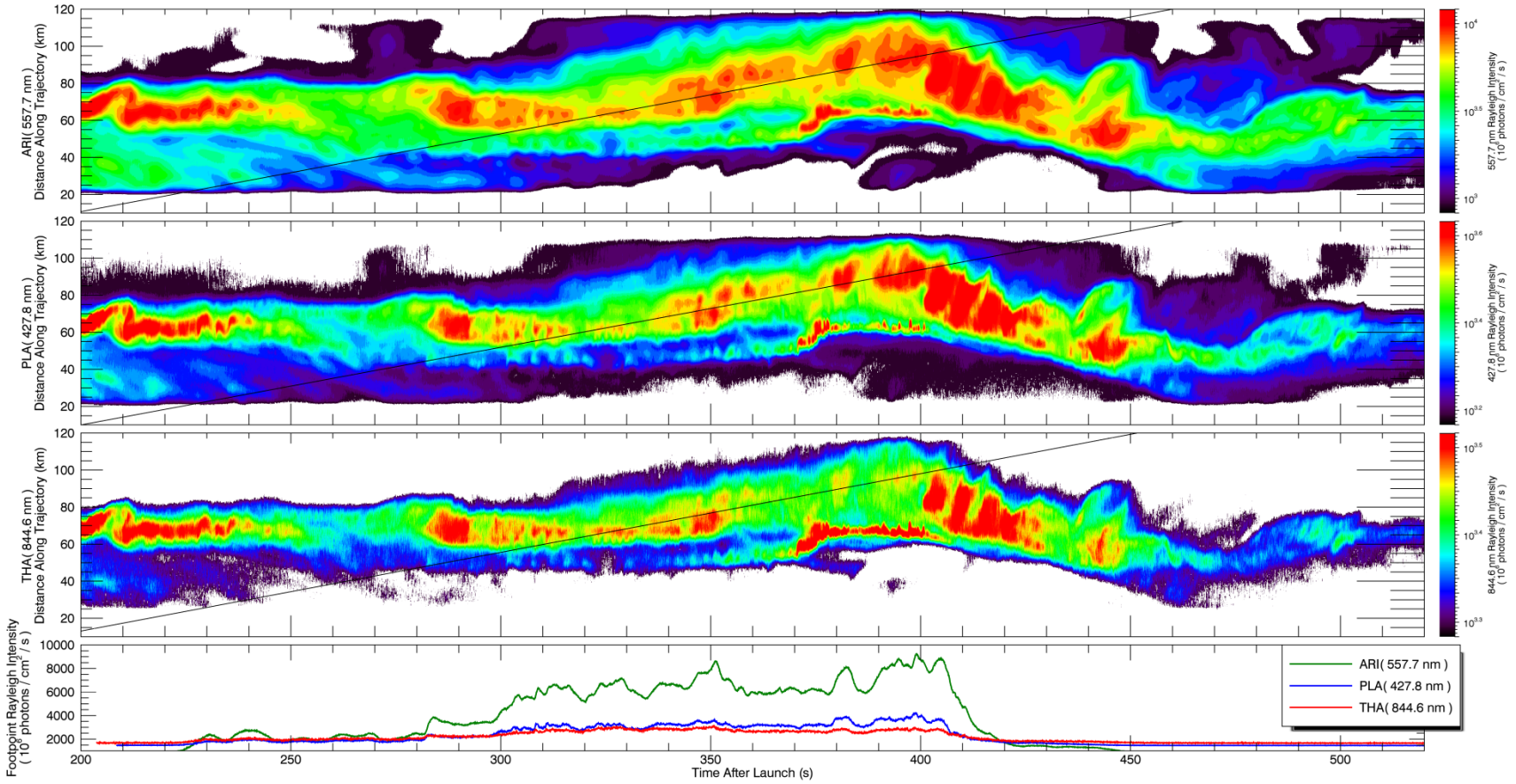
ARI(557.7 nm)
Distance Along Trajectory (km)
PLA(427.8 nm)
Distance Along Trajectory (km)
THA(844.6 nm)
Distance Along Trajectory (km)
557.7 nm Rayleigh Intensity
(10^6 photons / cm^2 / s)
427.8 nm Rayleigh Intensity
(10^6 photons / cm^2 / s)
844.6 nm Rayleigh Intensity
(10^6 photons / cm^2 / s)
Footpoint Rayleigh Intensity
(10^6 photons / cm^2 / s)
ARI(557.7 nm)
PLA(427.8 nm)
THA(844.6 nm)
Time After Launch (s)

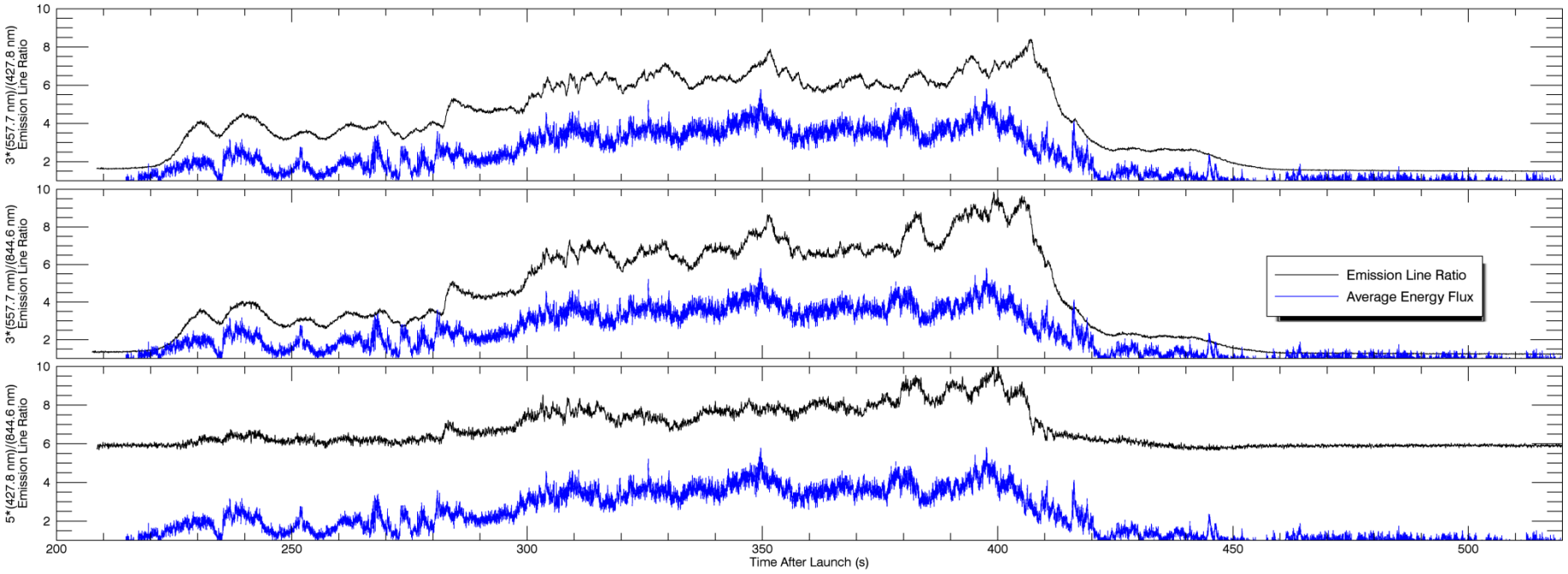
3*(557.7 nm)/(427.8 nm) Emission Line Ratio
3*(557.7 nm)/(844.6 nm) Emission Line Ratio
5*(427.8 nm)/(844.6 nm) Emission Line Ratio
Emission Line Ratio
Average Energy Flux
Time After Launch (s)

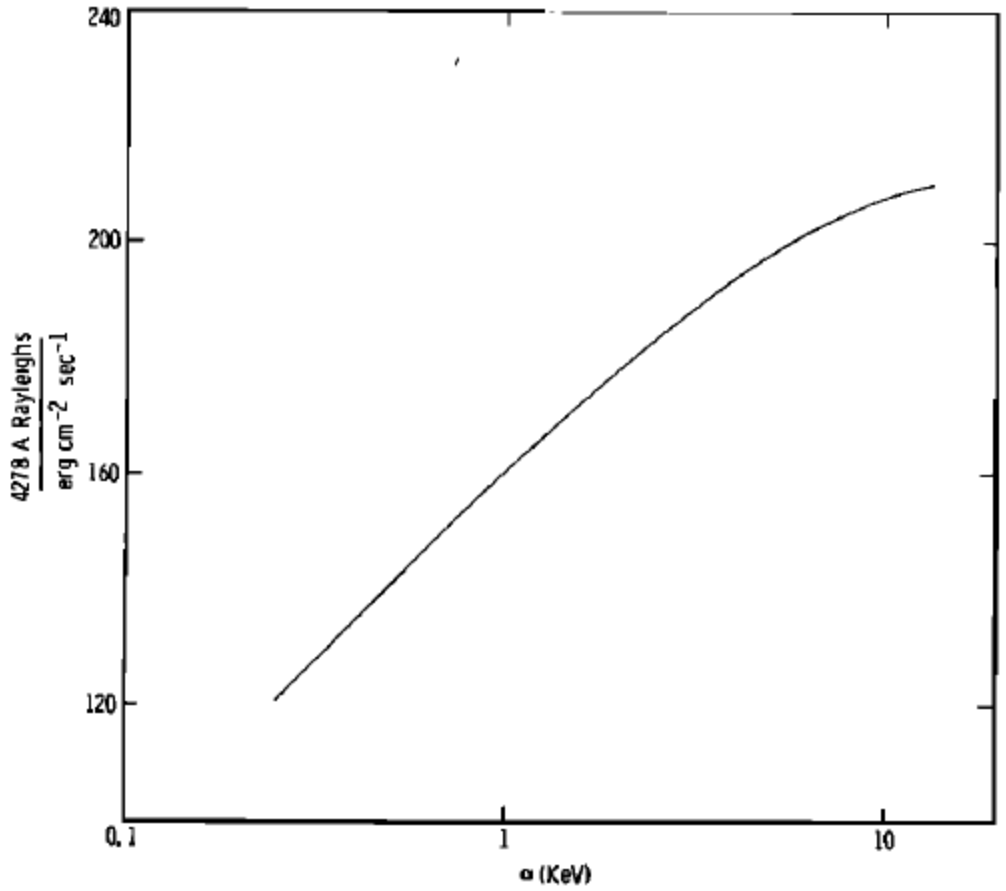

Fig. 7. Emission rate of 4278-Å radiation per unit energy deposition rate as a function of the characteristic energy α associated with the electron precipitation.

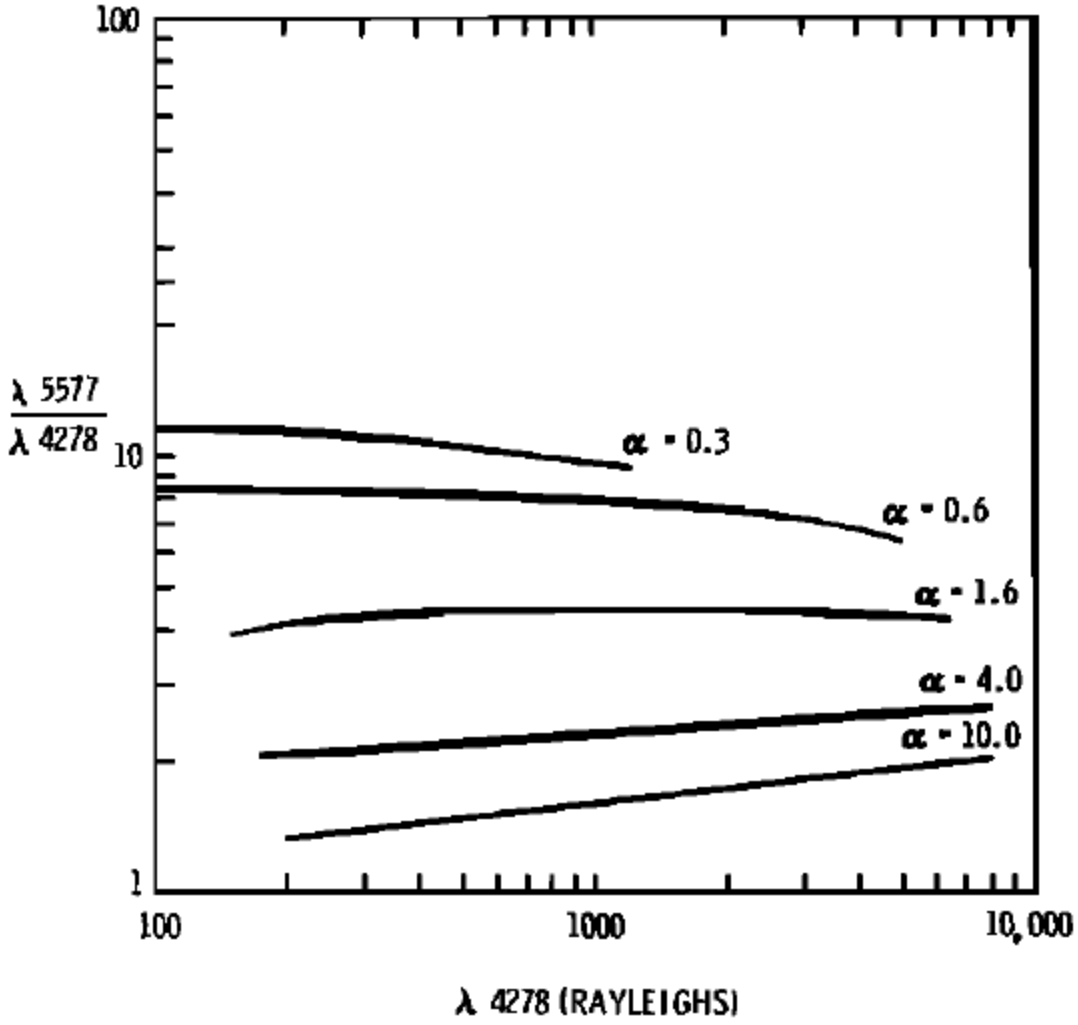
100
λ 5577
λ 4278
10
1
α = 0.3
α = 0.6
α = 1.6
α = 4.0
α = 10.0
100
1000
10,000
λ 4278 (RAYLEIGHS)

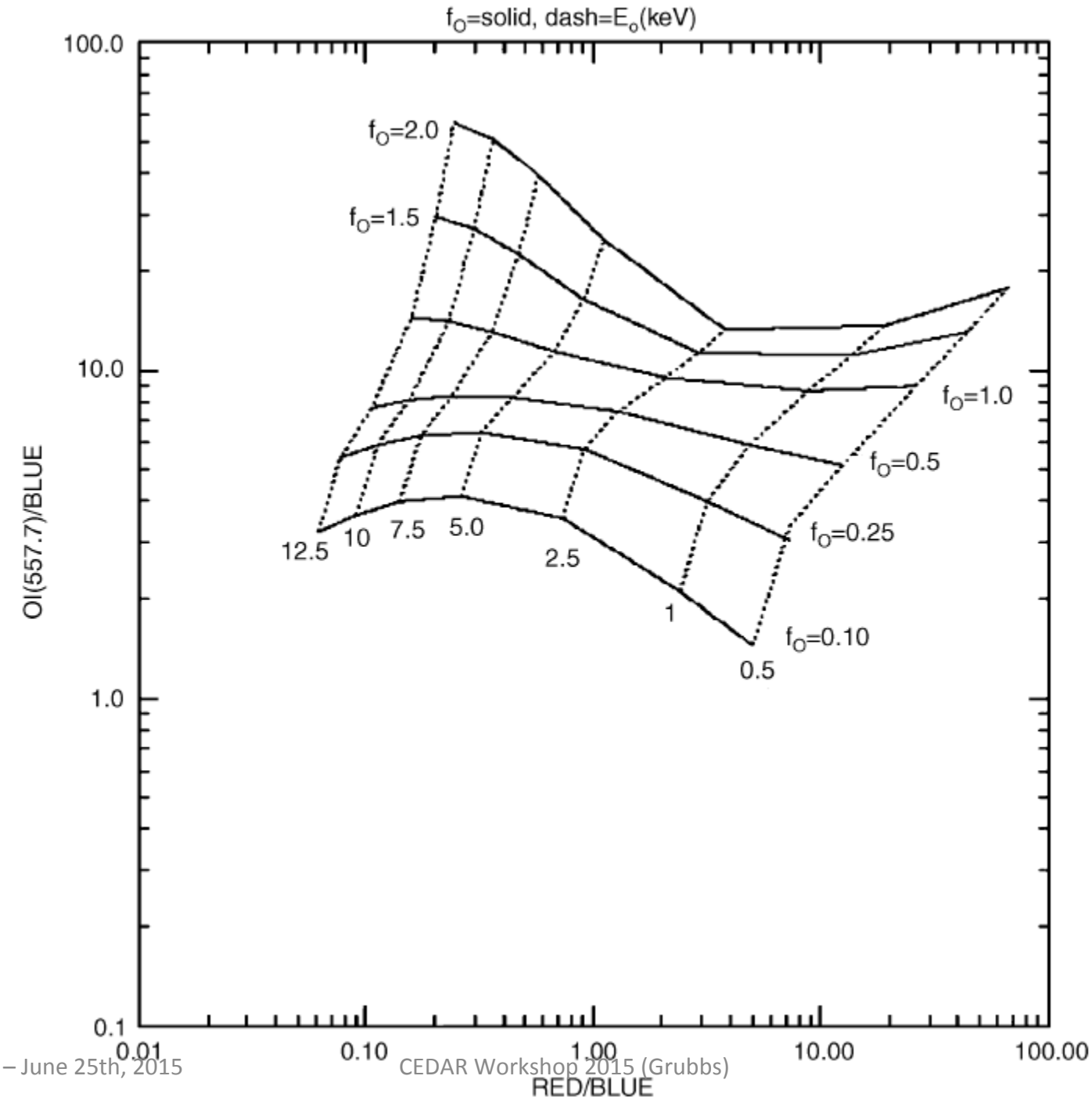
f_O=solid, dash=E_o(keV)
100.0
10.0
1.0
0.1
OI(557.7)/BLUE
f_O=2.0
f_O=1.5
f_O=1.0
f_O=0.5
f_O=0.25
f_O=0.10
12.5
10
7.5
5.0
2.5
1
0.5
0.01
0.10
1.00
10.00
100.00
RED/BLUE


SwRI
UCB-SSL
36.287
GREECE
Samara
USAFA
Southampton
Tromso
PFRR
KEO
Calgary
Cornell
GREECE 36.287 Samara
NASA - WFF
NSROC
UAF/GI

Image Thresholding

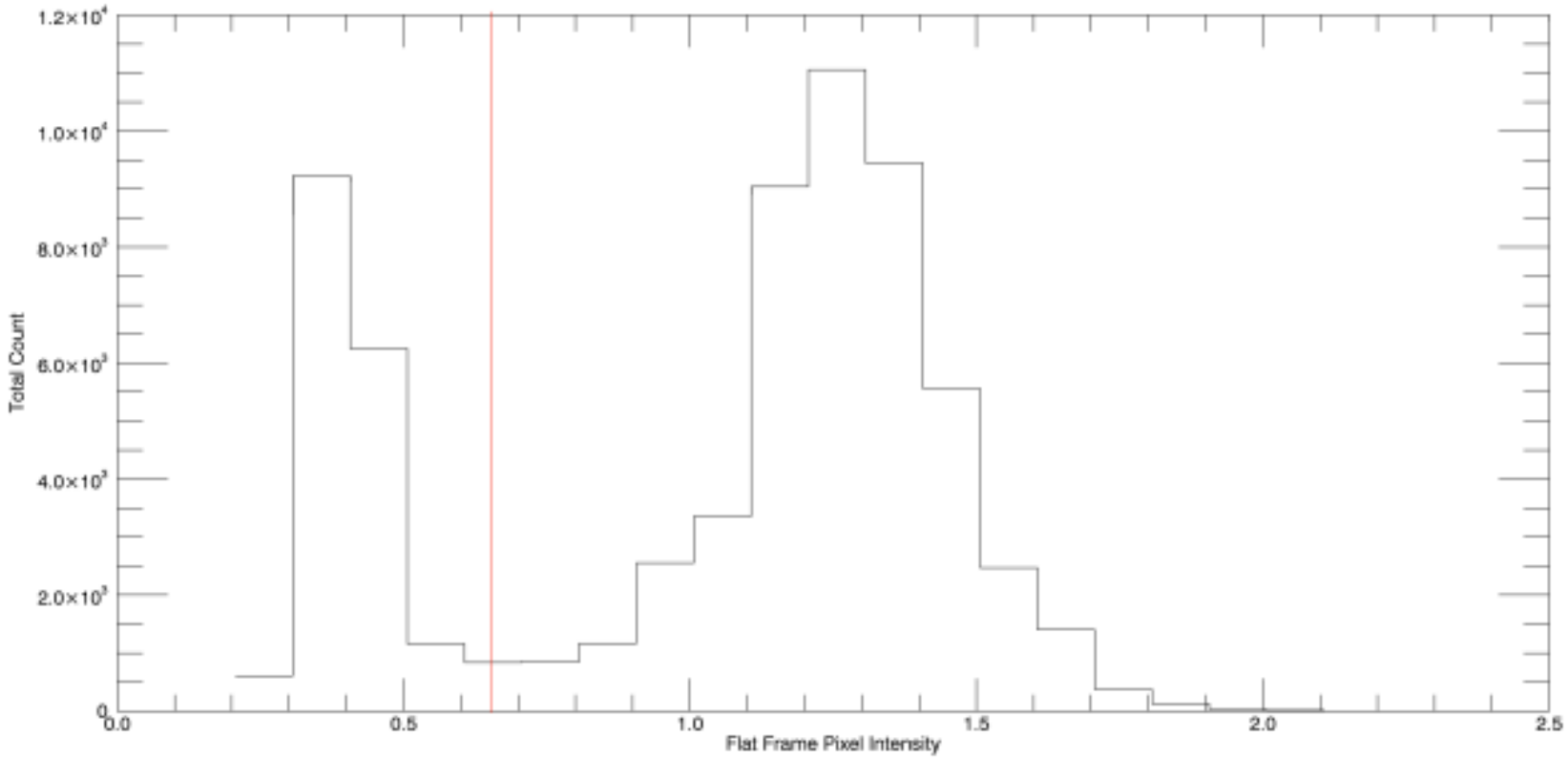

Flat-Fielding

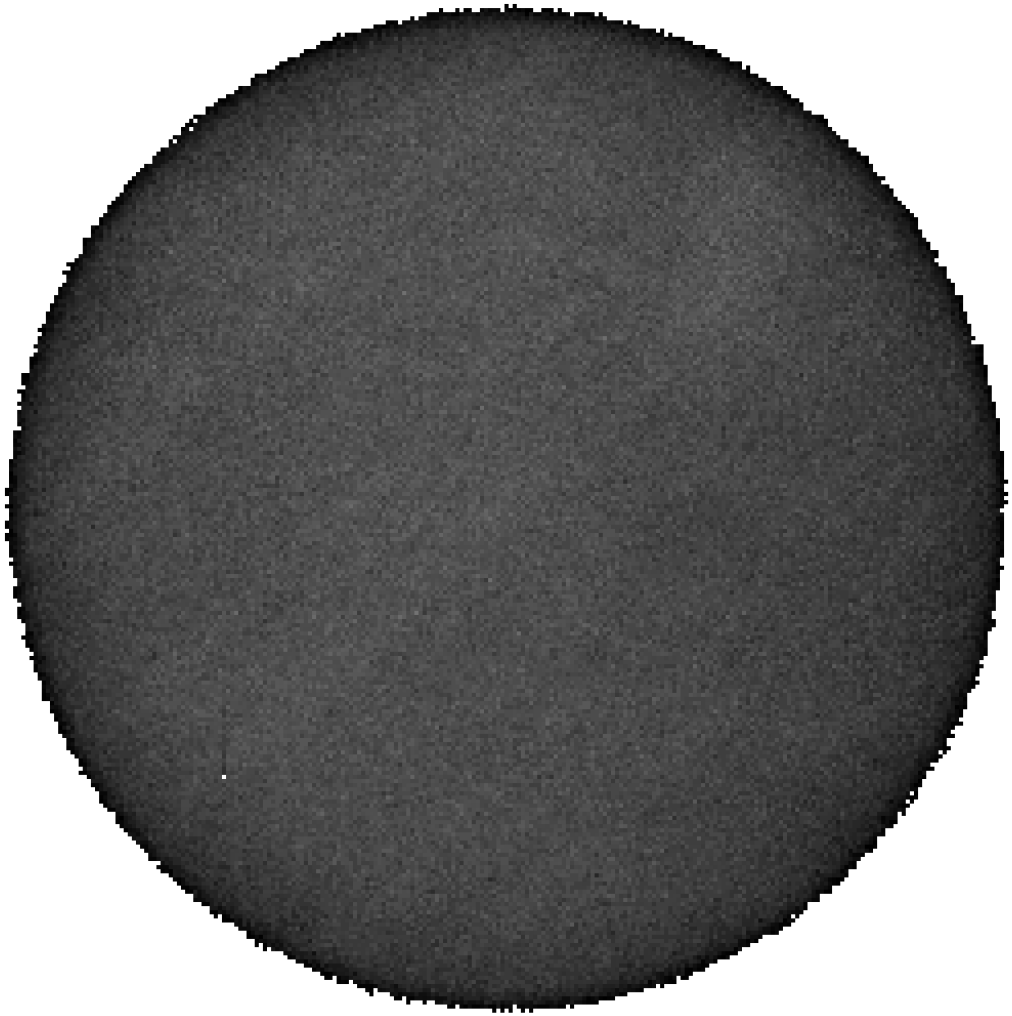

Abstract

- The aim of this research is the development a technique for the periodic and systematic calibration of ground-based imagers during deployment. Imagers experience a reduction in quantum efficiency as electronics decay from use over time. In addition, random events (cosmic rays or bright ambient light) may change characteristics of the detector in a short period of time. It important for each mission using these instruments to have a common system of units (Rayleighs or photon flux) for cross-comparison as well as self-comparison over time as decay occurs. With the advancement in technology, the quantum efficiency and signal-to-noise ratio of these imagers has improved so that stars within the field-of-view may be used for calibration. Background subtraction, flat-fielding, star-mapping, and other common techniques are combined in deriving a calibration technique appropriate for a variety of ground-based imager missions. These techniques take quantum efficiency, field-of-view, and wavelength filtering into account during calculations.

Scientific Motivation

- Ionosphere/Magnetosphere Interaction
  - Small scale structures
    - Formation/Cause
  - Auroral acceleration region
    - Acceleration mechanism
- Electron energy prediction
  - Electron transport models
    - Rees and Luckey, Strickland/Hecht et al., and Khazanov (Physical)
  - Model verification
    - In-situ and ground-based measurement comparison

Outline

- Background - GREECE
  - MOOSE Imagers
  - GREECE Rocket
- Methodology
  - APES Calibration
  - Auroral Photometry
- Results
  - Star Calibration
  - GREECE/MOOSE Comparison
- Discussion

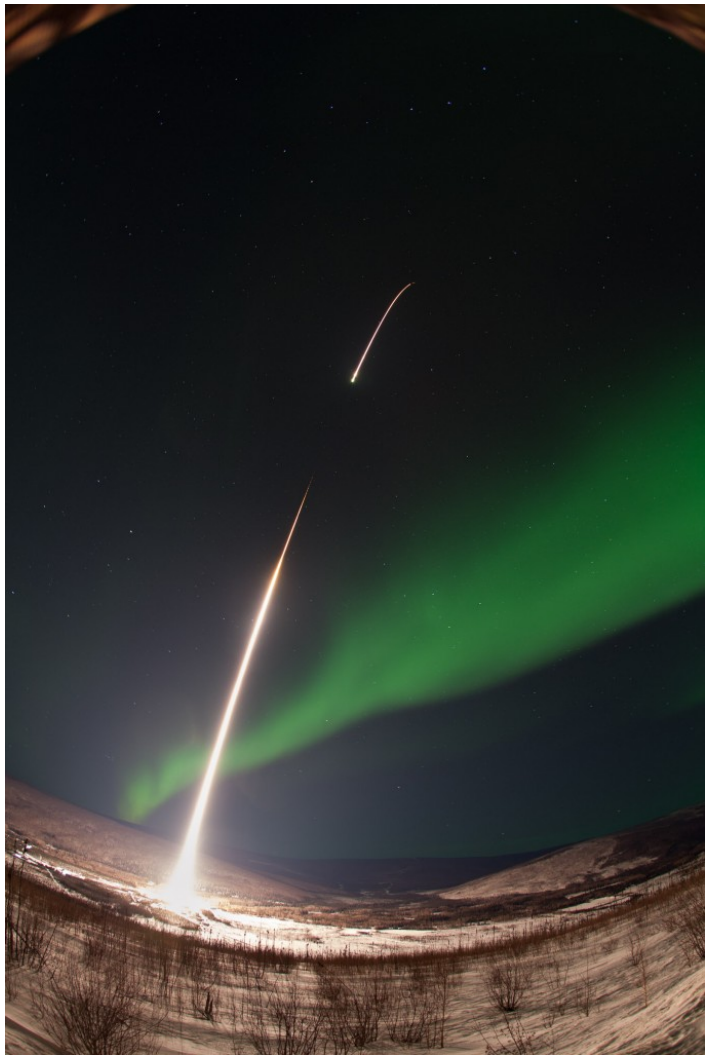

Background – GREECE Mission

- **G**round-to-**R**ocket **E**lectrodynamics-**E**lectrons **C**orrelative **E**xperiment

Imager	λ filter (nm)	Source	e^- characteristics
PLA	427.8 (Blue)	N_2^+(1N)	$\propto$ Total Energy Flux
ARI	557.7 (Green)	O	e^- Energy $\geq$ 10 keV
N/A	630.0 (Red)	O	e^- Energy $\leq$ 1 keV
THA	844.6 (Infrared)	O	e^- Energy $\leq$ 1 keV

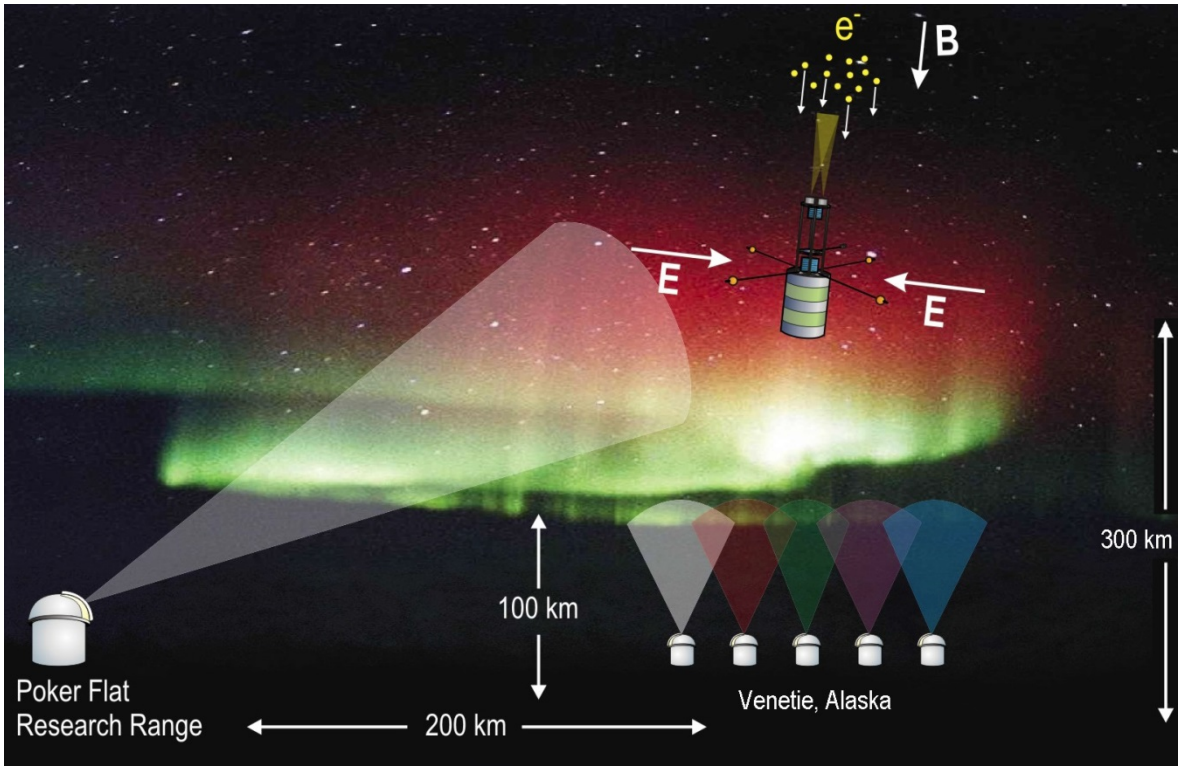

- High time resolution, multispectral, 2-D:
  - EMCCD Technology
  - Narrow-band filters (2 nm)
- Photometry
  - Measurement of light intensity/flux
- Mesoscale
  - Structures ranging approximately one to several hundred kilometers
- Precipitation Estimates
  - In-situ electron energy prediction